



# Spatio-temporal behaviours of tropical cyclones over the bay of Bengal Basin in last five decades

Manas Mondal <sup>a</sup>, Anupam Biswas <sup>a</sup>, Subrata Haldar <sup>a</sup>, Somnath Mandal <sup>a</sup>, Subhasis Bhattacharya <sup>b</sup>, Suman Paul <sup>a,\*</sup>

<sup>a</sup> Dept. of Geography, Sidho Kanho Birsha University, Purulia, W.B India

<sup>b</sup> Dept. of Economics, Sidho Kanho Birsha University, Purulia, W.B India

Available online 27 November 2021

## Abstract

Present research is an endeavour to scrutinise the spatio-temporal climatic characteristics of tropical cyclones (TCs) bustle in the Bay of Bengal basin, found in RSMC-IMD data all through 1971–2020. A large number of TCs, i.e. 121 with a decadal average of 35.2 TCs has been examined for the last 50 years where depression (D) and deep depression (DD) have not been taken into account as these are less violent in nature. During the study periods, inter-annual and inter-decadal variation in cyclogenesis, landfall, length, speed, track shape and sinuosity, energy metrics and damage profile have been perceived. The study is clearly showing TCs took the northward track during the pre-monsoon season and made their landfall across the coasts of Bangladesh and Myanmar, while post-monsoon TCs made their landfall directly on the coasts of Orissa and West Bengal. In the post-monsoon phase, VF, ACE and PDI are significantly higher than in the monsoon season in the case of TCs and higher in the pre-monsoon season than in the monsoon season in the case of TCs comparing the energy metrics in different seasons. TC activity is comparatively pronounced during La Niña and El Niño regimes respectively and the genesis position in the BoB is moves to the east (west) of 87° E. During the cold regime, the number of extreme TC above the VSWS category, increased intensely. It is believed that the research findings will help stakeholders of the nation to take accurate strides to combat such violent events with persistent intensification.

© 2021 The Shanghai Typhoon Institute of China Meteorological Administration. Publishing services by Elsevier B.V. on behalf of KeAi Communication Co. Ltd. This is an open access article under the CC BY-NC-ND license (<http://creativecommons.org/licenses/by-nc-nd/4.0/>).

**Keywords:** Tropical cyclones; RSMC-IMD; Cyclogenesis; Energy metrics; La Niña and El Niño

## 1. Introduction

North Indian Ocean (NIO) accounts for almost 8 per cent of all tropical cyclones that originate across the globe and almost 75 per cent of the genesis of NIO TCs were produced in the Bay of Bengal (BoB) basin (Pandey and Liou, 2020) and a

spotlight has been paid to the studies of the Bay of Bengal cyclonic activity as more than 60 per cent of global causalities have been encountered from this cyclogenesis basin with intense rainfall, terrestrial flooding and high storm surge (Singh et al., 2001a, 2001b; Wang et al., 2017; Mousavi et al., 2010). Several exceptionally serious super cyclones have occurred in the Bay of Bengal basin over the past two decades, causing more significant damages, due to large storm surges (in the case of Aila in 2009 and Sidr in 2017), low coastal areas (in the case of Odisha Super Cyclone in 1999, Hudhud in 2014 and Bulbul in 2019) inadequate identification along with socio-demographic vulnerability (in case of Giri in 2010, Phailin in 2014 and Amphan in 2020). For cyclones such as Fani, Amphan (Down To Earth, 2020; The Hindu, 2020), prediction and behaviors of cyclonic landfall have been considered close

\* Corresponding author.

E-mail address: [suman.krish.2007@gmail.com](mailto:suman.krish.2007@gmail.com) (S. Paul).

Peer review under responsibility of Shanghai Typhoon Institute of China Meteorological Administration.



to accurate, prediction and behaviors of cyclonic landfall have been seen to be broader in present day forecasting (Karmakar and Hassan, 2004; Pandey and Liou, 2020). Despite the formation of these cyclonic routes and its landfall, millions of people fled across the globe due to loss of immovable property, loss of livestock, and loss of livelihood. From 1990 to 2017, the lesser due to weather-related catastrophe rose dramatically from 0.22 per cent of global GDP to 0.42 per cent of global GDP, and the peak was 0.48 per cent in 2006 (<http://ourworldindata.org/natural.disasters>). Focusing on Aila cyclone (2009) in BoB basin, approximately 150,000 communities were homeless and 100 of river embankments were violated in coastal West Bengal and Bangladesh due to storm surge of 6 m–8m height, nearly 50,000 ha of agricultural land were lost due to storm surge triggered embankment breaching with salt water intrusion at a cost of us \$ 26.3 million. In coastal Orissa, Fani was another cyclone that seriously affected 750 km of roads, 267 culverts with more than 25,000 street lights destroyed. This phenomenon has been estimated to include a provisional report on damage accounted for US\$ 8.1 billion. Over the last two decades, the BoB basin has witnessed more badly impacted tropical cyclones, causing big losses in the share of state and national GDP as well as climate-induced migration (Fig. 1).

**Table 1** summarises the tropical storm characteristics of 121 cyclonic storms over 50 cyclonic storm seasons for the Bay of Bengal basin during the last 50 years (January 1970 to November 2020). More recently, on May 20, 2020, at a record 18 h of 240 km/h (at a mean sustained wind intensity of >220 km/h), cyclone Amphan transformed into a super cyclone due to the Bay of Bengal recorded surface temperature of 32 °C–34 °C before the cyclone. Such rapid intensification was experienced last year in the NIO basin and super shift a cyclone due to ocean warming temperature and turned an extremely serious cyclone into a super cyclone and thus further intensification and quantification of seasonality, with its shape and energy, decadal scenario of cyclonic events are needed.

## 2. Background

Most of the study targets have been developed conventionally to classify the spatial and temporal history of cyclonic events in various ocean basins, emphasizing physical characteristics (Bhardwaj and Singh, 2019; Wang et al., 2017) and social risk assessment (Cutter and Finch, 2008; Marín-Monroy et al., 2020) with such review is directly related to the hazard and its risk correlation with severity (Oo et al., 2018; Rabby et al., 2019). However, focus has also been given to figure out the meaning and shifting form of track form over the last decade (Terry and Feng, 2010; Terry and Kim, 2015). Cyclone also took a twisting course and for forecasting the landfall site and mitigating steps, the trajectory evaluation and forecast are gaining tremendous importance (Zhang et al., 2013; Terry and Gienko, 2018). Such cyclonic track shape or sinuosity is also influenced by the warm ocean and recently these cyclonic track shape shifts in the warm ocean with its length (Emanuel, 2005; Pandey and Liou, 2020). For instance, in 2019, the extremely

intense cyclonic storm Fani (3 min sustained wind 215 m/h) took a sharp bend from the Andhra coast (India) to Odisha (coast) due to rapid intensification in a sea surface temperature ranging 30 degrees–31 degrees C and low vertical wind shear. As a result, 72 people were killed in Odisha, with an estimated US\$ 1.74 billion in damage. Several areas of Bangladesh have been found to be inundated, damaging 63,000 ha of farmland in 35 districts. It has been known that the more curvature-shaped tropical cyclones try to persist for a longer duration, thereby causing more damage. Terry and Gienko (2011) have developed a technique to assess track sinuosity, and researchers have experimented with a significant change in shape quantification over the last 5 years (Colbert and Soden, 2012; Terry and Kim, 2015).

Several studies have documented the warming impact of global warming on the surface of the ocean. The required condition for the formation of TCs is 26°C–27 °C temperature, and based on NOAA-SST results, Pattanaik (2005) showed an increase in the NIO basin of 0.5–0.6° c/100 years. The cyclones thus become even more intensified (Fani, Bulbul, Amphan) with high mean sustain wind (MSW) proportionate to tropical cyclone energy matrices (velocity flux, cumulative cyclonic energy and PDI) in a very short period of time and benefit high mean sustain wind (MSW). ACE has accounted for the frequency and duration of tropical cyclones and PDI indicates the severity of TCs. These cyclone indices give a strong indicator of SST rise with storm intensification over the NIO basin (Emanuel, 2005; Mohapatra and Kumar, 2015). Since the BoB basin has a strong bi-modal cyclonic activity, ACE and PDI are high in the primary peak post-monsoon season and lower in the secondary peak pre-monsoon. As argued by many researchers for the BoB basin (Sengupta et al., 2007; Singh, 2008; Ng and Chan, 2012), these energy induces have a direct association with La-Nina (Nino 3–4 SST anomaly) with an intensification in this sense to examine spatio-temporal activity of tropical cyclonic storms (category I to V as per IMD) originating in the Bay of Bengal basin during 1971–2020. In further, thorough review was addressed.

India, Bangladesh and Myanmar, situated in the Bay of Bengal (BoB), have been found to be immensely influenced by cyclonic activities with bi-modal peaks during the year. Globally, nearly 7% of total cyclones were created by this BoB basin, but the loss was estimated to be nearly 50–60% of global damage to lives and property (Liou et al., 2017; Kumar et al., 2016). In compliance with the United Nations, during the last 30 years (i.e. 1990–2020) in the Indian subcontinent (only the eastern portion) almost US\$ 5.2 trillion was estimated to have been lost due to cyclone-induced risk. The loss was severely affected by the overall high population density, shallow BoB basin form, high tidal range with poor coastal security and overall fragile social fabric (Lindeboom et al., 2012; Rehman et al., 2020). The spike in sea surface temperature, higher tidal acceleration and submergence of the Bengal Delta worsened the condition during the last 20 years specifically (Sahana et al., 2019; Sahana and Sajjad, 2019). Rather recently, the intensification of cyclones like Fani, Bulbul and Amphan strongly illustrates the changing nature of cyclonic strength

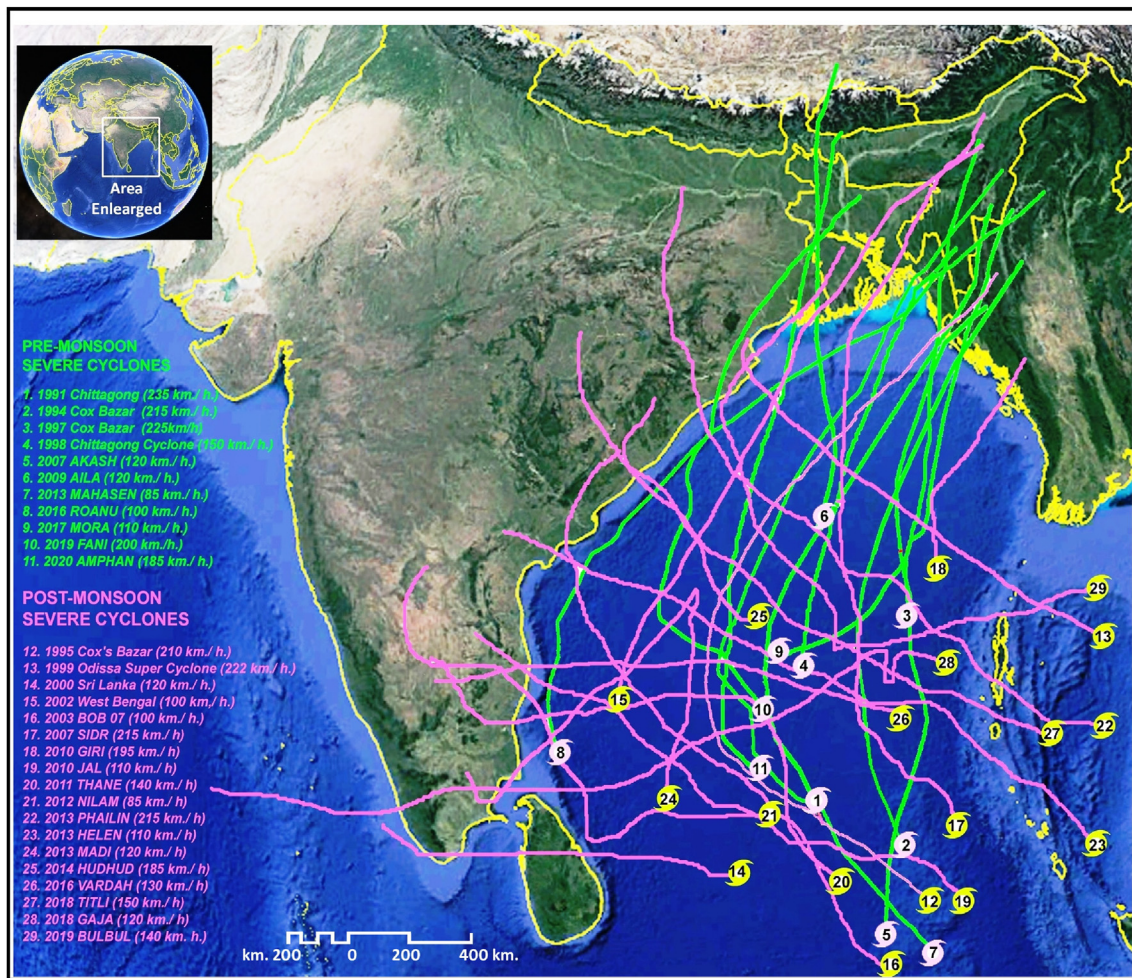


Fig. 1. Severe Cyclonic Tract during 1991–2020 in Pre-monsoon and Post-monsoon seasons.

Table 1

Summary of tropical storm characteristics for Bay of Bengal basin, from January 1970 to November 2020 (50 Cyclonic Storm seasons and n = 176).

Parameter	Median	Mean	Range
Decadal Frequency (no.)	36	35.2	30–41
Cyclogenesis Lat. (°)	89°25'	90°08'	78°09' – 113°33'
Cyclogenesis Long. (°)	11°58'	12°43'	2°11' – 21°40'
Landfall Lat. (°)	87°33'	86°54'	78°01' – 101°28'
Landfall Long. (°)	19°42'	18°21'	10°02' – 22°34'
Duration (hour)	83	94.4	15–276
Distance Covered (km.)	1091.5	1195.2	28.6–4111.4
Speed (km.)	85.00	99.22	45.0–260.0
Minimum Pressure (mb.)	988	980.5	912–1008

**Source:** Computed by Authors from RSMC-IMD e-Atlas.

**N.B.** Analysis has been done on the track data for the tropical cyclone phase (sustained wind speed over 3 min  $\geq 85$  km), i.e. here we have excluded the weaker depressions formed and finished of cyclones.

with its destructive effects. These warm waters and intensification of cyclone create tremendous rainfall within a very short period of time, causing coastal floods, dam breaches and saline water infiltration into agricultural land and fish farms. The damage of 1.3 trillion US dollars in the last two years (i.e. 2019–2020) indicates the essence of the damaging capacity of the recent developed cyclonic storms and that the backward

socio-economic coastal community faced climate-induced displacement as a result (Siddiqui, 2014; Fang et al., 2014; Chen and Mueller, 2018).

The present research thus aims to investigate the actuality and origin of spatio-temporal tropical cyclones with track form and cyclonic energy related problems. In addition, as global warming and sea surface temperature have induced basic cyclonic storms to become serious, ENSO phenomena have also been cautious to consider the relationship of origin and energy-related problems. While this proposition in this study deliberates numerous meteorological problems, it does not examine any climatic consequences.

### 3. Study region and materials

#### 3.1. Study region

The World Meteorological Organisation (WMO) designates a Regional Designated Meteorological Centre (RSMC) based in New Delhi to track tropical cyclones formed in the North Indian Ocean (NIO) basin under the supervision of India Meteorological Department (IMD) and to establish an archive of cyclonic events. The RSMC area of responsibility (AoR)

stretches to eastern Africa with the Arabian Peninsula on the western coast and the western coast of the Thai-Malay peninsula on the eastern coast of the peninsula (Fig. 2). This NIO basin has been broken into two sub-basins: a) the eastern Bay of Bengal (BoB) basin and b) the western Arab Sea (AS) basin.

The research seeks to analyse the spatio-temporal activity of tropical cyclones over the BoB basin over the past 50 years (i.e. 1971–2020). The basin was formed as a funnel stretching from 50°N (near Sri Lanka and the southern part of the Andaman and Nicobar Islands) to West Bengal (India) and the coastal region of Bangladesh (nearly 22°N) with Myanmar to the east and the coast of Orissa and Andhra to the west. This coastal region is densely populated with key subsistence opportunities for agriculture and fisheries. Temperature increasing, cyclone intensification and increases in the number of cyclonic days have subjected such a socio-economic backward community to a much more precarious situation.

### 3.2. Materials

The date of Tropical cyclone data are obtained directly from Cyclone E-Atlas of the online RSMC-IMD ([rsmcnewdelhi.imd.gov.in](http://rsmcnewdelhi.imd.gov.in)) portal for tropical cyclones over the basin of the North Indian Ocean. After registration, RSMC-IMD databases are publicly accessible on the web portal and very easy to view and even in downloadable format (.pdf,.xml,.gif formats). Tropical cyclone datasets include the name of the cyclone, the date and place of origin and landfall, the length of the cyclone, the seasonal character, the maximum strength of wind and the energy matrix. The complete datasets, sorted in detail according to the purposes of the analysis after uploading, have been discussed in the following portion. The origin of the dataset used in this research was shown in Appendix (Table 1).

## 4. Methodological overview

Both cyclonic incidents from 1971 to 2020 were mainly sorted out as the nature of magnitude as recommended by IMD. In this analysis, Depression (D) and Deep Depression (DD) were not examined as these are the prevalent phenomena in the Indian subcontinent. Only cyclonic incidents with a wind speed of 62 km/h have been taken into consideration. 121 tropical cyclones (Cyclonic Storm-CS, Severe Cyclonic Storm-SCS, Very Severe Cyclonic Storm-VSCS, Very Severe Cyclonic Storm-ESCS and Super Cyclonic Storm-SuCS) were considered after the exclusion of D and DD incidents for further analysis.

In the next step, with their intensity, all tropical cyclones (i.e. 121 TCs) were graded according to months, seasons and decadal trend. In the ARC-GIS platform, cyclogenesis and landfall of all cyclonic storms have been plotted to approximate the type of origin as well as the influence on locations of landfall. The present research therefore analyses the cyclonic case tract from 1971, which was much older than the satellite period, and this may result in some kind of less precision in statistical measurements (Pandey and Liou, 2020; Schreck et al., 2014).

In order to approximate the track sinuosity character of 121 tropical cyclones during 1971–2020, additional cyclogenesis and landfall sites have been plotted (Fig. 3a–d). In GIS Program (ESRI ARC-GIS Platform), 121 TCs were digitized to calculate the sinuosity of the cyclonic track with the real distance traveled and the straight distance in the measuring instrument. The ratio was determined to obtain the sinuosity value after getting the geodesic value of the curved and straight distance occupied by each cyclone. The converted sinuosity index value was subsequently determined with the sinuosity

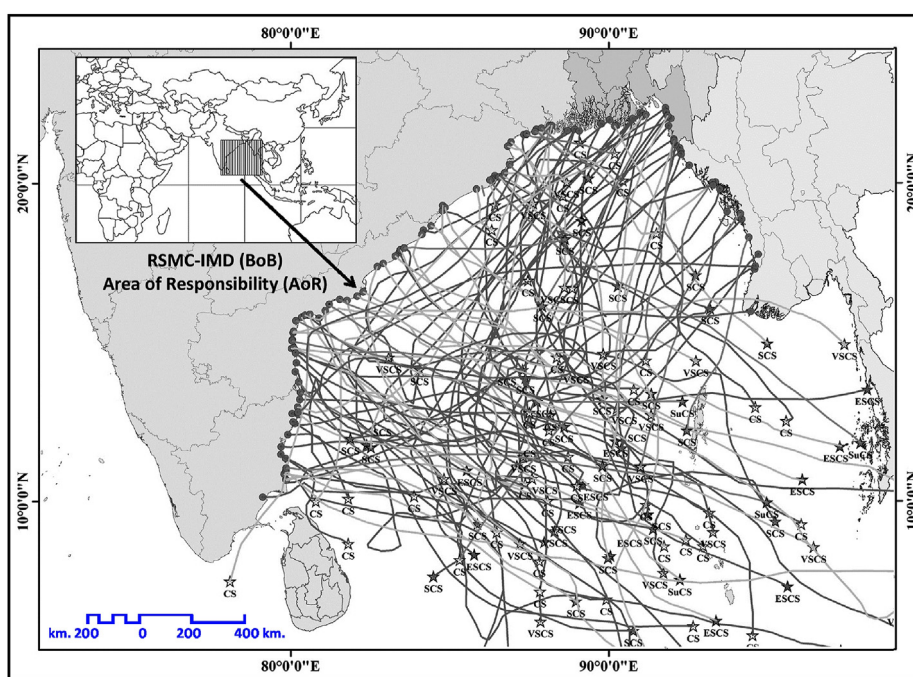


Fig. 2. The RSMC area of responsibility (AoR).

value using the following translation function. (Pandey and Liou, 2020; Terry and Gienko, 2011):

$$SI = \sqrt[3]{(S - 1)} \times 10$$

where, S represents the measured sinuosity of the particular track and SI represents the transformed sinuosity index value. When SI value is found '0' it is logical that the cyclone has been a straight one.

Different energy matrixes correlated with tropical cyclones, i.e. velocity flux (VF), cumulative cyclone energy (ACE) and power dissipation index (PDI) were measured in the next step with linear pattern analysis for seasonal variation and time period. These data have been analysed by means of the RSMC-IMD web portal for the years 1970–2020. In addition, the cyclonic trend and ENSO phenomenon are associated with the cyclonic energy matrix and in La Niña years this has a strong sign of higher energy level than that in El Niño years (Girishkumar et al., 2015; Nath et al., 2016; Bhardwaj et al., 2019). The National Oceanic and Atmospheric Administration (NOAA) has created the Oceanic Niño Index (NIO) to classify the 3-month mean sea surface temperature (SST) events of El Niño (warm periods) and La Niña (cool periods)

for the Niño 3.4 region. In this analysis, the Niño 3.4 region dataset for 1981–2020 was taken into account as RSMC-IMD energy matrix datasets have a data constraint and authors are only able to access the 1982–2020 energy matrix dataset.

## 5. Results and discussion

### 5.1. Spatial and temporal distribution of cyclonic storms

#### 5.1.1. Annual and decadal distribution

Fig. 3 shows the origins (cyclogenesis) and landfall (cyclosis) of tropical cyclones ( $msw > 34$  knots) between 1971 and 2020. These TCs were formed in various parts of the BoB basin and produced cyclosis in different parts of India (Tamil Nadu, Andhra Pradesh, Orissa and West Bengal) with Bangladesh, Myanmar and Sri Lanka. In the Bay of Bengal Basin, the locations of the Tropical Cyclone (TC) genesis occur in a wide segment between latitudes from  $5^{\circ}\text{N}$  to  $22.5^{\circ}\text{N}$  and longitudes from  $80^{\circ}\text{E}$  to  $95^{\circ}\text{E}$ . Fig. 3, according to its concentration, expresses TC genesis locations in different sections, color-coded by the index of concentration. The longitudinal isolation of the region of TC formation is captured by the

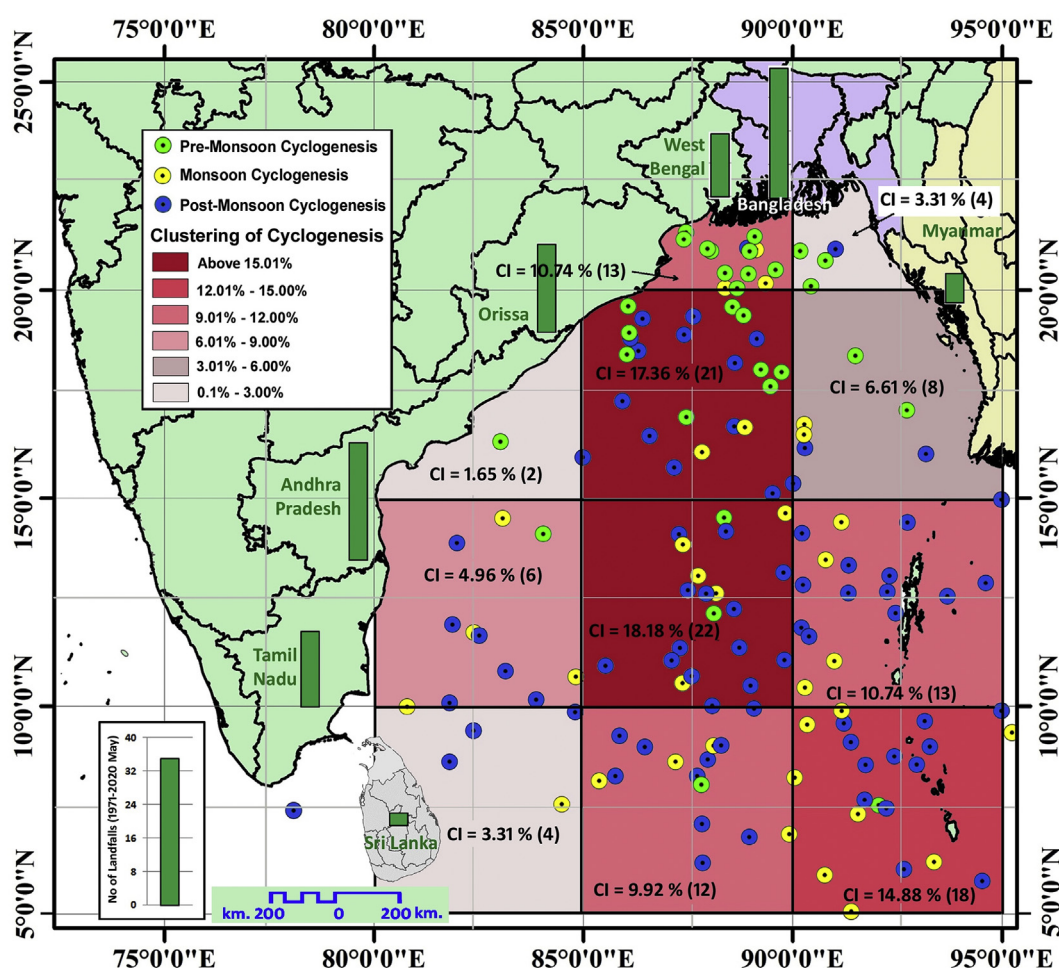


Fig. 3. Genesis of tropical cyclones in Bay of Bengal basin during 1971–2020.

clustering of TC genesis sites. Clusters have been discussed beginning from the west (from 80°E.) to the Myanmar coastal area (95°E.).

With 1.65% of all cyclones, Sri Lanka's genesis section displays the least number of concentrations over the last 50 years. The largest concentration has been found within 85°E–90°E and 10°N–15°N. With 18.18 per cent (genesis of 22 TCs) and another cluster of 21 TCs (17.36 per cent) have been found within 85°E–90°E and 15°N–20°N. More than 25 per cent (31 TCs) of TCs sources with the position of 900E–95°E was identified by another field concentration of Tropical Cyclones (Table 2) 5°N–15°N and 5°N–15°N 90°E–95°E and 5°N–15°N (within Andaman and Nicobar Islands).

The locational analysis of the genesis of TCs offers an understanding of the probable type of TC track, as the genesis path significantly improves the track, speed, distance cover and decay of the TCs. The tracks of TCs curved and landfall with enormous destructive force into the soil floor in the post-monsoonal season. In the direction of the eastern ward, most of the pre-monsoon Tropical Cyclones turn or curve and strike the coast of Bangladesh. In the event of recent devastating cyclones, SIDR (2006), Aila (May 2009), Fani (2019), Bulbul (2019) and Amphan (May 2020) have made landfall on the shores of Bangladesh and India, respectively. This unique character of the cyclonic landfall has changed over the last 15–20 years, which is a very interesting point of study. In the case of a decadal environment, CS and SCS have decreased in number, while VSCS, ESCS and SuCS have increased in number (Table 3). This finding indicates that the effect of global warming on the BoB basin is a good predictor (Wang et al., 2017; Bhardwaj and Singh, 2019).

#### 5.1.2. Seasonal and monthly variation in cyclonic storms

Table 4 and Table 5 demonstrate the seasonal and monthly history of Tropical Storms in the BoB basin during 1971–2020. The occurrence of TCs was found to be high in number and formed during the post-monsoon era in the lower and middle part of the BoB following the westward route (Fig. 4). The occurrence of TCs increases significantly during the pre-monsoon season with a shift of the location of their source to the north and rapid intensification of the BoB basin discovered by intense cyclonic storms. The TCs led the northward path and landed on the coasts of Bangladesh and Myanmar, while the post-monsoonal TCs landed in Orissa and West Bengal (Fig. 4).

Table 2

Genesis of tropical cyclones in Bay of Bengal basin during 1970–2020 (up to June).

Location of genesis of TCs	Act. (in %)	Location of genesis of TCs	Act. (in %)	Location of genesis of TCs	Act. (in %)
80°E. - 85°E.		85°E. - 90°E.		90°E. - 95°E.	
20°N. - 25°N.	–	20°N. - 25°N.	13 (10.74)	20°N. - 25°N.	4 (3.31)
15°N. - 20°N.	2 (1.65)	15°N. - 20°N.	21 (17.36)	15°N. - 20°N.	8 (6.61)
10°N. - 15°N.	6 (4.96)	10°N. - 15°N.	22 (18.18)	10°N. - 15°N.	13 (10.74)
5°N. - 10°N.	4 (3.31)	5°N. - 10°N.	12 (9.92)	5°N. - 10°N.	18 (14.88)

Source: Computed by Authors from RSMC-IMD e-Atlas.

Table 3

Decadal Pattern of Cyclonic events according to severity in BoB Basin.

Decades	Cyclonic Storm (CS: km)	Severe cyclonic storm (SCS: km)	Very severe cyclonic storm (VSCS: 119–165 km)	Extremely severe cyclonic storm (ESCS: 166–220 km)	Super cyclonic storm (SuCS: > 220 km)
1971–1980	9	6	7	1	1
1981–1990	4	16	4	3	2
1991–2000	8	5	7	3	2
2001–2010	9	6	3	3	0
2011–2020	8	3	6	3	1

Source: Computed by Authors from RSMC-IMD e-Atlas.

Nevertheless, the origin of monsoonal TCs have dramatically decreased and shifted northward towards the head of the BoB basin during the latter part of the study period. The post-monsoonal TCs developed in the BoB basin throughout the entire period of the study and seriously influenced the collapse of the ground on the eastern coast of India with greater magnitude of impact. Relevant variations in the year-round formation of TCs were found in the BoB basin between 1971 and 2020. During the October–December season, the most intense cyclonic storms evolved and, on the other hand, almost similar trends were observed during the April–May months. In the BoB basin, the genesis of TCs clearly shows the bi-modal situation. During the months of the monsoon, lower storm categories such as D, DD and CS were created from June to September throughout the study period. It has been noticed during the entire study period that can weather conditions can be experienced only in four (04) TCs in the month of January, February, March, July and August.

During 1971–2020, Fig. 5a–d validates the seasonal and monthly cyclogenesis trend of Tropical Storms in the BoB basin. The incidence of TCs was observed in high numbers during the post-monsoon period and established in the southern parts of the BoB and followed the westward pathway. The frequency of TCs rises steadily during the pre-monsoon season with a change in their origin positions to the north, and the extreme cyclonic storms discovered rapid BoB basin intensification. The northward route was pursued by the TCs and landed on the coasts of Bangladesh and Myanmar, while the post-monsoonal TCs landed in Orissa and West Bengal. Nonetheless, during the latter part of the study period, the origin of the monsoonal TCs substantially decreased and

Table 4

Seasonal Pattern of Cyclonic events according to severity in BoB Basin.

Seasons	Cyclonic Storm (CS: 62–88 km)	Severe cyclonic storm (SCS: 89–118 km)	Very severe cyclonic storm (VSCS: 119–165 km)	Extremely severe cyclonic storm (ESCS: 166–220 km)	Super cyclonic storm (SuCS: > 220 km)
Pre-monsoon (Mar–May)	6	7	8	4	3
Monsoon (June–Sept.)	12	3	1	0	0
Post Monsoon (Oct.–Dec.)	20	26	18	9	3

Source: Computed by Authors from RSMC-IMD e-Atlas.

Table 5

Monthly Pattern of Cyclonic events according to severity in BoB Basin.

Months	Cyclonic Storm (CS: 62–88 km)	Severe cyclonic storm (SCS: 89–118 km)	Very severe cyclonic storm (VSCS: 119–165 km)	Extremely severe cyclonic storm (ESCS: 166–220 km)	Super cyclonic storm (SuCS: > 220 km)	Total
January	1	0	0	0	0	1
February	0	1	0	0	0	1
March	0	0	0	0	0	0
April	2	1	0	1	1	5
May	4	6	8	3	2	23
June	7	1	1	0	0	9
July	1	0	0	0	0	1
August	1	0	0	0	0	1
September	2	2	0	0	0	4
October	8	11	4	5	1	29
November	7	12	9	2	1	31
December	5	3	5	2	1	16
Total	38	37	27	13	6	121

Source: Computed by Authors from RSMC-IMD e-Atlas.

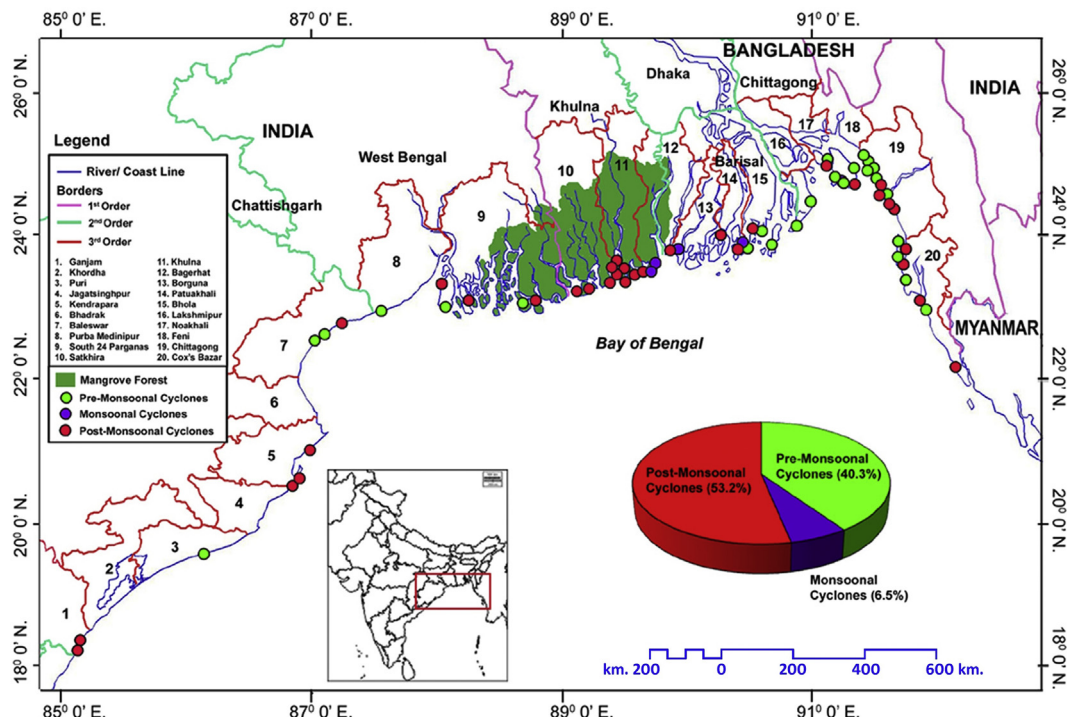


Fig. 4. Major landfalls in pre-monsoon and post monsoon during 1970–2020.

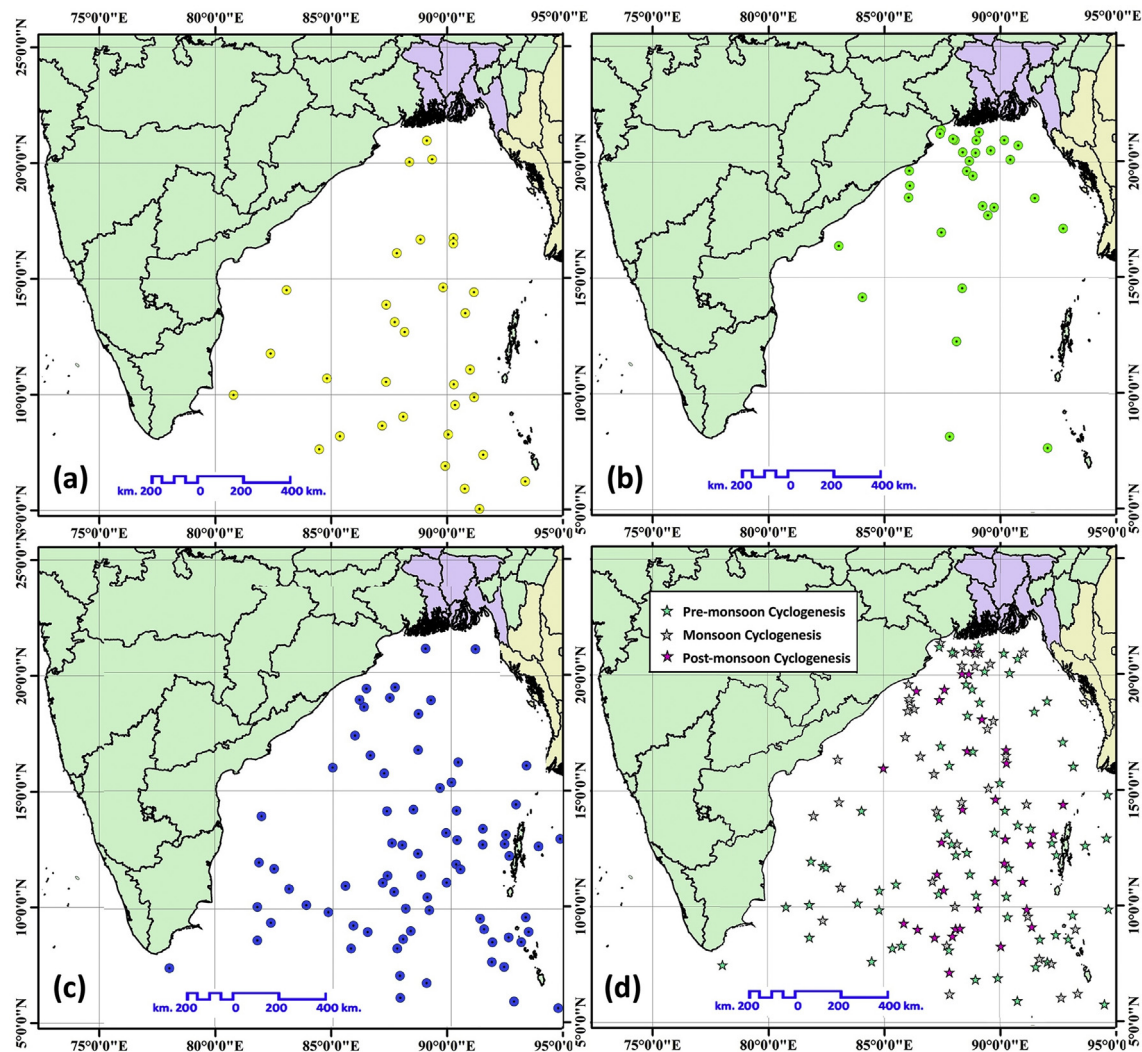


Fig. 5. Cyclogenesis in different times during 1971–2020 (a) pre-monsoon, (b) monsoon, (c) post-monsoon and (d) annual.

Table 6  
Number of TCs of different intensity in BoB Basin during 1982–2020.

ENSO Phenomena	Cyclonic Storm	Severe cyclonic storm	Very severe cyclonic storm	Extremely severe cyclonic storm	Super cyclonic storm
El Niño Years (14 Years)	8	9	5	4	1
La Niña Years (16 Years)	15	10	8	5	2
Neutral (9 Years)	6	12	8	4	1
Total (39 Years)	29	31	21	13	4

Source: Computed by Authors from RSMC-IMD e-Atlas.

moved northward towards the head of the BoB basin. The post-monsoonal are formed along the BoB basin throughout the entire span of analysis and the ground fall on the eastern coast of India has been severely affected by higher damage severity.

### 5.1.3. Cyclonic pattern and ENSO phenomena

Many scholars have studied the correlation in between El Niño-Southern Oscillation (ENSO) and Bay of Bengal (BoB) tropical cyclones. As statistically driven seasonal forecasts of tropical cyclonic activity in the western North Pacific use ENSO as one of the key predictors, the relationship is of obvious interest. The location of cyclogenesis and the total number of tropical cyclones have been the subject of several studies. The main focus here is on the impact of ENSO on the strength of tropical cyclones. In recent years, several scientists have paid attention to the issues between ENSO manifestations and TC movement (e.g., quantity, TC movement, origin, pathway and strength). The North Indian Ocean alone accounts for about 7% of global TCs, with a frequency that varies from four to five times compared to that in the Arabian Sea, higher in the Bay of Bengal (BoB) (Anandh et al., 2020; Balaguru et al., 2016; Biswas and Kundu, 2018). Recently, efforts have been concentrated on optimization to determine the connection between ENSO and BoB TCs (Neumann, 1993; Dube et al., 1997). In addition, due to ENSO, modulated BoB TCs

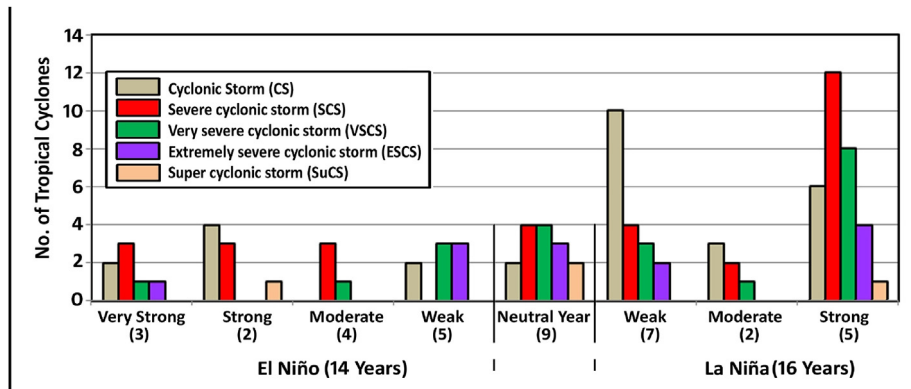


Fig. 6. Tropical Cyclones in different ENSO phase during 1982–2020 Note: Figures within the parentheses are no of years under ENSO phenomena.

activities can cause catastrophic devastation after landfall on the low-lying topography along the coastline with high population density. In this segment, the universal unit used by NOAA in the tropical Pacific to identify cases of El Niño (warm) and La Niña, the Oceanic Niño Index (ONI) was used (cool). For the Niño 3.4 zone, it is the 3-month median SST anomaly that runs for 5° N–5°S and 120°–170°W. Occurrences are defined as 5 consecutive alternate 3-month periods at or above the +0.50 anomaly for warm (El Niño) events and at or below the –0.5 anomaly for cold (La Niña) events. The threshold is then divided into events like Low (0.5–0.9 SST anomaly), Moderate (1.0–1.4), Extreme (1.5–1.9) and Very Strong (1.5–1.9). In order to grade an event as mild, moderate, high or very strong in the sense of this study, the threshold must have been equal to or exceeded three consecutive three-month periods of overlapping.

Here, we researched the intensity tropical cyclones in El Niño, La Niña and neutral years over the BOB basin during 1982–2020 (Table 6). During El Niño, out of 26 tropical cyclones, 8 are CS, 9 are SCS, 5 are VSCS, 4 are ESCS, and 1 is SuCS. In this phase 15 are CS, 10 are SCS, 8 are VSCS, 5 are ESCS and 2 in SuCS category. It is evident that more extreme cyclonic events are observed in La Niña years compared to El Niño and neutral years, and the amount of TCs in the BOB basin during 1982–2020 have been provided (Fig. 6). The

findings provide strong agreement with many researchers (Lander, 1994; Wang et al., 2017) in agreement with the favourable state of thermodynamics and vortices prevailing over the BOB basin due to the shift in SST in the eastern part of the Indian Sub-continent. The yearly dispersal during the La Niña and El Niño years of TC cases of different categories (CS-SCS and VSCS-SUCS) is shown in Table 6. During the 1982–2020, in BoB, 60 TC cases from CS-SCS and 38 have been recorded from severity cases (VSCS-SUCS). 10 out of 25 (40) and 15 out of 25 (60 per cent) TCs were formed during the warm and cold years, respectively (Table 6). On average, during the cold (1.05 TC cases per season) regime, the number of TC cases (CS-SUCS) is almost 1.5 times of that of the warm (0.71 TC cases per season) regime. If we consider only the TC events of SUCS class, 2 TCs occurred under the cold regime and 1 occurred under the warm regime.

In different ENSO phases, broad spatial variations are evident in the genesis sites, tracks and landfall patterns of TCs (Fig. 7a and b). While most of the formation of peak season TCs is concentrated between 5°–15° latitudes; however, a longitudinal swing can be clearly seen in their place of genesis. Around two-thirds of the overall TCs during the years of La Niña and El Niño years shaped eastward and westward respectively. The mean genesis position of TCs is 89°, 55'E and 10°, 42'N during the El Niño years, while it is 90°, 10'E and

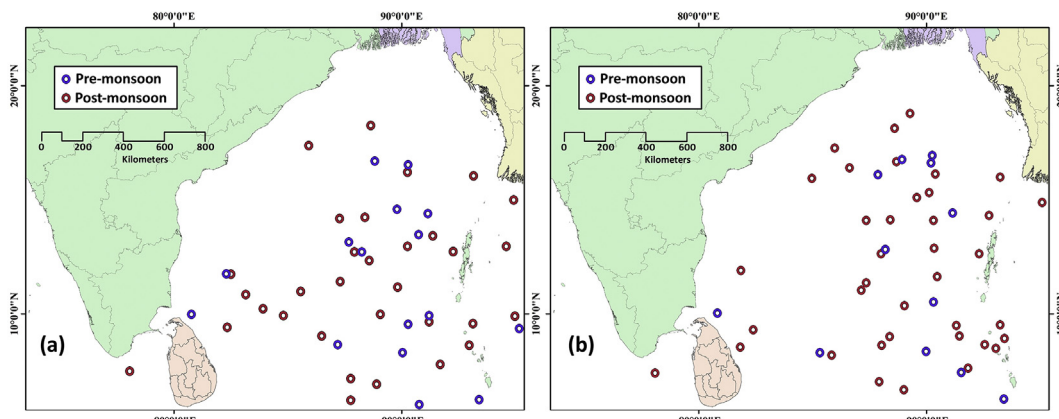


Fig. 7. Cyclogenesis of TCs in pre-monsoon and post-monsoon seasons at different ENSO phase during 1982–2020 (a) El Niño and (b) La Niña.

9°40'N in the La Niña years. Before landfall, the TCs of La Niña years must travel great distances and attain a mature point, and vice versa in El Niño years. In La Niña, the lifespan of TCs is greater than that in El Niño. The mean number of TC days per year in La Niña (8.92 days) is considerably higher than that in El Niño (4.51 days). The longer life is also a possible cause of greater ability and intensification of TCs over BoB in the La Niña years and it is prominent in the case of AMPHAN (May 2020). During El Niño and La Niña, the mean numbers of landfall of TCs is 0.52 and 0.79 per year, respectively. Of the total landfall of TCs, about 83 per cent travel westward During El Niño years, and they make landfall at the south of 170 N over the eastern coast of India as also suggested by Bhardwaj et al. (2019). In comparison, about 73 per cent of the overall landfall of TCs curved northwest and northward in the years of La Niña and hit north of 18°N over India, Bangladesh and Myanmar's eastern coast.

## 5.2. Energy metrics associated with tropical cyclones in BoB

### 5.2.1. Temporal pattern of energy metrics

A new analysis has been undertaken to evaluate the phenomenon in inter-annual variety in TCs metrics along with velocity flux (VF), accumulated cyclonic energy (ACE) and power dissipation index (PDI) bearing in mind the inverse dynamics of TC recurrence over the BoB basin in distinctive seasons and year as a whole to find out whether they have comparable variety as that of TC recurrence or like that of TCs recurrence similar that of SST. The lifetime of TC is used to measure TC behaviour by season. The ACE, also known as the potential for TC disaster, is aligned with the evolution of the existence of

large-scale climate in accordance with customary, including various large-scale features. As loss is correlated with the cube of wind speed over the entire storm area, PDI is a TC hazard metric. Although the ACE accounts for both the intensity and duration, the PDI places more emphasis on TC gravity. The assessment of trends in the intensity, duration and severity of TCs, as well as the potentially to harm and failure due to TCs across the sector, will therefore be one of the main implications of this study. To examine the impact of climate change on the operation of TCs, these indices are also considered significant.

The annual Mean Velocity Flux is about  $16.24 \times 10^2$  kt (Table 7) over the Bay of Bengal basin amid a year for the tropical cyclones. In this way VF over the Bay of Bengal basin is within the proportions of 5.1:1, 5.3:1, 5.7:1 and 6.1:1 for pre-monsoon, monsoon, post-monsoon and annual time frame respectively against the proportion of recurrence of TCs. So, the ratio of VF is not in the agreement with the proportion of recurrence, because it too depends on the term and escalation of TCs. When inter-seasonal varieties are considered, due to the higher frequency, duration and usual concentration of TCs in the post-monsoon season, the VF of TCs is essentially higher in the post-monsoon and pre-monsoon. In several seasons over the Bay of Bengal basin during the entire study period, there is an essential contrast in the mean VFs. Evaluating the VFs over the Bay of Bengal basin (Table 7), in the pre-monsoon and post-monsoon seasons, as well as in the case of TCs, the sway is essentially higher over the year as an entire. The fact that the average VF essentially depends on the number, length and intensity of TCs may be due to the fact that they are higher than BoB. As the frequency and length of TCs are lower during this season, the VF for TCs is less influential over the BoB in the rainstorm season (monsoon season).

Table 7

Mean velocity flux ( $\times 10^2$  kt), Mean accumulated cyclone energy ( $\times 10^4$  kt $^2$ ) and Mean power dissipation index ( $\times 10^6$  kt $^3$ ) over Bay of Bengal (BOB) Basin during 1982–2019.

Seasons	Energy Matrix	Mean	$\delta$	C.V.	Min	Max	Mean TC
Pre-Monsoon	Mean velocity flux (VF)	4.87	5.84	120.03	0.00	20.25	0.95
	Mean accumulated cyclone energy (ACE)	6.58	21.69	329.62	0.00	133.88	
	Mean power dissipation index (PDI)	2.81	4.71	167.40	0.00	16.42	
Monsoon	Mean velocity flux (VF)	0.79	1.66	210.74	0.00	7.50	0.15
	Mean accumulated cyclone energy (ACE)	0.36	0.86	238.70	0.00	4.53	
	Mean power dissipation index (PDI)	0.18	0.52	291.24	0.00	3.06	
Post-Monsoon	Mean velocity flux (VF)	10.18	8.42	82.64	0.00	39.50	1.79
	Mean accumulated cyclone energy (ACE)	6.80	7.12	104.72	0.00	28.58	
	Mean power dissipation index (PDI)	5.32	7.04	132.44	0.00	29.41	
Annual	Mean velocity flux (VF)	16.24	9.58	58.98	0.45	48.55	2.66
	Mean accumulated cyclone energy (ACE)	10.66	8.10	75.99	0.20	38.98	
	Mean power dissipation index (PDI)	8.36	8.32	99.46	0.09	41.85	

Source: Computed by Authors from RSMC-IMD e-Atlas.

The mean accumulated cyclonic energy (ACE) over the BoB is roughly  $10.66 \times 10^4 \text{ kt}^2$  for the TCs (Table 7). Concurring to Mohapatra and Kumar (2015), based on 1990–2013 results, the ACE over the NIO was approximately  $9.5 \times 10^4 \text{ kt}^2$ . Therefore, the results of this research indicate that in recent years there has been a sharp slope in ACE over the BOB. In this way, for pre-monsoon, monsoon, post-monsoon and annual time periods, ACE over the Bay of Bengal Basin is within the ratio of 6.9:1, 2.4:1, 3.8:1 and 4.1:1, respectively, against the ratio of TCs recurrence. Considering the inter-seasonal variety of ACE in respect to TCs, it is entirely higher over the BoB basin in pre-monsoon and post-monsoon than in the monsoon season. The stronger ACE over the BoB basin in the post-monsoon season may be due to the clear stage of the ENSO bolting process and seasonal activity of TCs as ENSO peak stages appear to occur at the end of the calendar year, i.e. in the middle of October–December and TC genesis is higher over the ACE in the post-monsoon season (Oct–Dec). It is essentially higher in pre-monsoon and post-monsoon when the ACE is connected to the BoB basin in different seasons (Table 7) as it were within the case of TCs. Considering the CV, it is 330, 239, 105 and 76 per cent per year over BoB for the ACE, thus shows broad inter-annual variety and confirming Chime et al. findings (2000). Due to the most extreme genesis frequency and concentrated TCs in the middle of this season and longer tracks, the inter-annual

changeability is minimum in the post-monsoon season over the BoB as seen from Fig. 1.

The mean PDI over the BoB basin is shown in Table 7 in different seasons and year as a whole. The mean PDI of TCs is about  $41.85 \times 10^6 \text{ kt}^3$  annually and  $16.42 \times 10^6 \text{ kt}^3$ ,  $3.06 \times 10^6 \text{ kt}^3$  and  $29.41 \times 10^6 \text{ kt}^3$  for pre-monsoon, monsoon and post monsoon respectively. In pre-monsoon and post-monsoon seasons, the PDI is essentially greater than that for TCs over the BoB as a whole in the monsoonal season. There is a comparison of the PDI on BOB for TCs as a whole for the year as well as VF and ACE for comparable purposes as assigned to the variety. The CV value is least in post-monsoon season likewise VF and ACE for all the TCs in BoB.

### 5.2.2. Energy metrics over BOB basin and relation with ENSO phenomena

The VF, ACE and PDI are marginally lower in the El Nino years (Fig. 6) than in the La Nina years and lower in the El Nino years than in the normal post-monsoon years in the BoB season. Additionally, there is no substantial change in energy metrics between La Nina and normal years over the BoB during the post-monsoon season (see Table 2 in Appendix). As a result, development of the El-Nino condition may mean lower than normal TC activity, whereas development of the La-Nina condition may not indicate higher than normal TC activity in terms of increased VF/ACE/PDI over the BoB post-

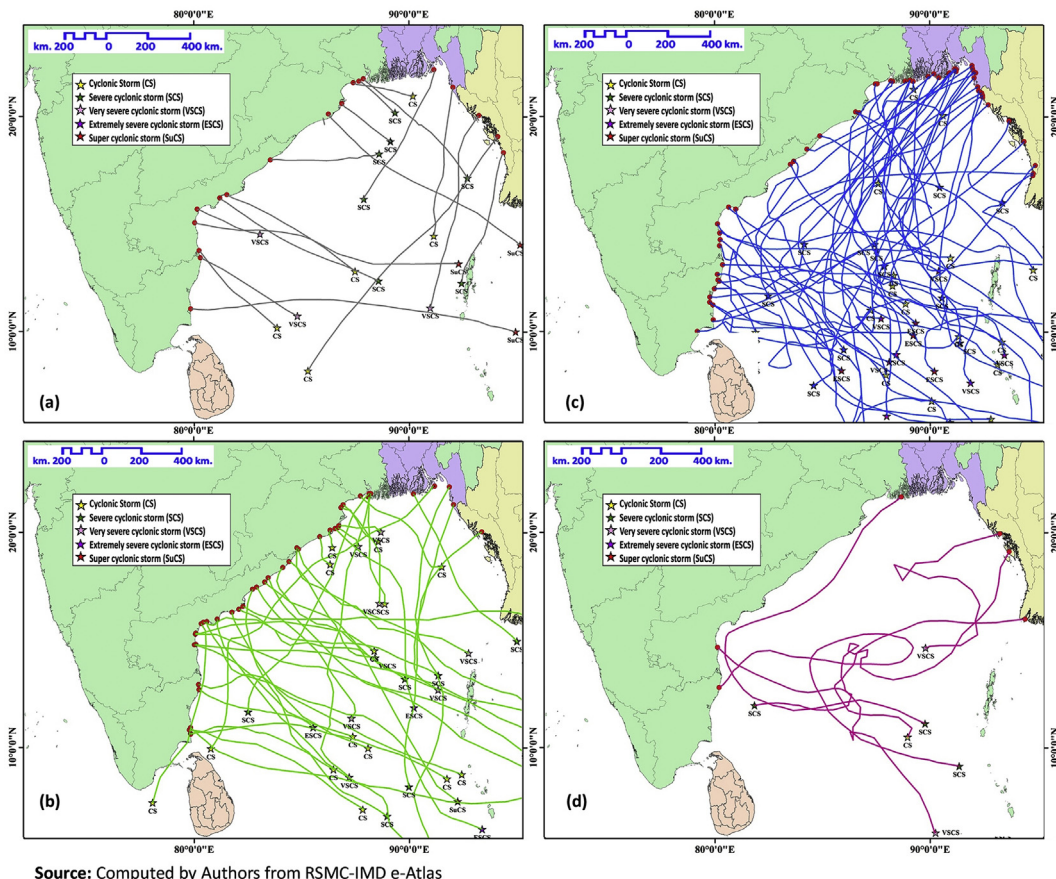


Fig. 8. Mean accumulated cyclone energy (ACE) and La Nino and El Nino Conditions in BOB.

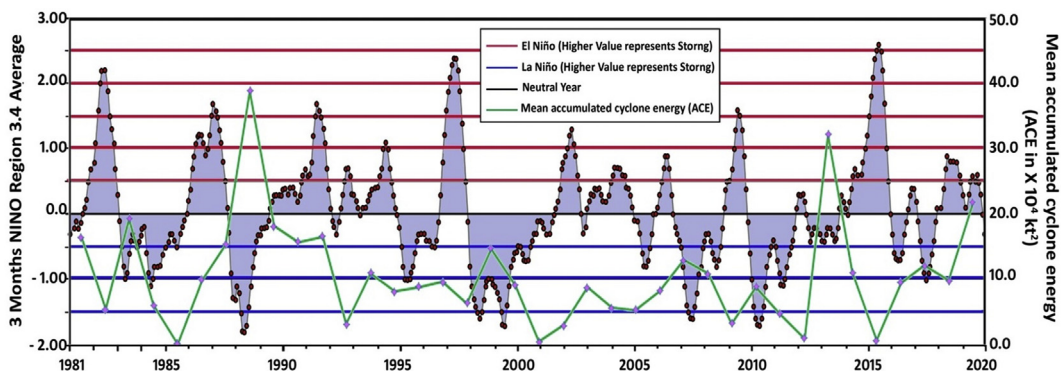


Fig. 9. Track shape of cyclones classified in (a) straight, (b) quasi-straight, (c) quasi-sinuous and (d) sinuous groups over BOB basin during 1971–2020.

Table 8  
Classification of sinuosity and track SI of cyclones in BoB basin during 1971–2020.

Quartile	Measured Sinuosity value (SI)	Track SI	Category Name	No of Cyclones
I	1.000–1.016	0.144–0.549	Straight	19
II	1.017–1.085	0.550–0.952	Quasi-straight	41
III	1.086–2.065	0.953–2.201	Quasi-Sinuous	55
IV	>2.065	>2.201	Sinuous	6

Source: Computed by Authors.

Table 9  
Sinuosity and Track SI of Cyclones during different seasons in BoB Basin during 1971–2020.

Parameter	Pre	Monsoon	Post	Annual
Measured Sinuosity	1.255	1.15	1.221	1.214
Track SI value (SI)	1.158	0.974	1.008	1.033
No. of Cyclones	42	36	98	176

Source: Computed by Authors from RSMC-IMD e-Atlas.

monsoon season. There is no noticeable impact of El Niño/La Niña conditions on the energy metrics of TCs/CDs over the BoB for both the pre and post-monsoon seasons and the BoB during the pre-monsoon season. In reference to TCs 'ACE', it endorses the earlier results of Ng and Chan (2012). During the pre-monsoon, monsoon and post-monsoon seasons and year as a whole, the CC between Nino 3.4 SST anomaly and the VF/ACE/PDI over BoB was determined to further investigate the relationship between ENSO and ACE and the findings are provided in Fig. 8.

The reaction of TC activity over the BoB is just contrary to that of the Northwest Pacific, where, relative to other Ocean basins, increased TC activity occurs during El Niño years (Wang and Chan, 2002). The genesis of TCs over the northwest Pacific occurs relatively above the north latitude during El Niño years. The number of remnants traveling west-northwest/northwest ward from these TCs crossing the coasts of Vietnam/Thailand is smaller in the years of El Niño than in the years of La Niña. As a consequence, the genesis of TCs over the BoB is lower in El Niño years due to these remnants. The remains of TCs/CDs from the South China Sea are correlated with around

two thirds of the genesis of CDs above the BoB, according to Rao (1976). The BoB provides favourable divergence, greater moist static instability, increased convection (suppressed) and strong (low) heat capacity of tropical cyclones (TCHP) in the BoB (unfavourable).

### 5.3. Track shape and its pattern

Surface morphology of cyclone track applies to certain elements of track form calculation and quantification. Our track morphology method is based on track sinuosity, which is basically a function of how far a cyclone track 'meanders' from the least paths between the cyclogenesis and positions of cyclosis. It is easy to comprehend a sinuosity-based metric for track morphometry and makes inspection in a GIS setting and analysis using normal Tools for statistics. Relatively straight cyclone lines, twisted or more sinuous, are all readily quantified. The technique has been used successfully to investigate cyclone tracks in other ocean basins, including the North and South Pacific, the North Atlantic, and the western South Indian Ocean (Terry and Feng, 2010; Terry et al., 2013; Terry and Kim, 2015; Terry and Gienko, 2018). The essence of the cyclonic track in the BoB basin during 1971–2020 is clearly illustrated in Fig. 9, and all cyclones have been categorized into straight, quasi-straight, quasi-sinuous and sinuous groups (Table 8).

It is possible to investigate throughout the season from the available details changes in the form of tracks during 1971–2020. For each month within the study time span, the method here is to count the frequency of cyclones showing above or below normal (median) track sinuosity. In Table 9, the comparison indicates that cyclones spawned in the early post-monsoon period (during October–November) appear to follow more quasi-straight to quasi-sinuous tracks (46 per cent), in comparison to the pre-monsoon period in April–May (23 per cent). For other months of cyclogenesis, the proportions of straighter and more sinuous tracks are nearly similar as seen in post-monsoon period. The results for pre-monsoon and post-monsoon are notable because the pluralities of cyclones that have intensified into the Very severe cyclonic storm to super cyclone' category have traditionally been reported in these periods.

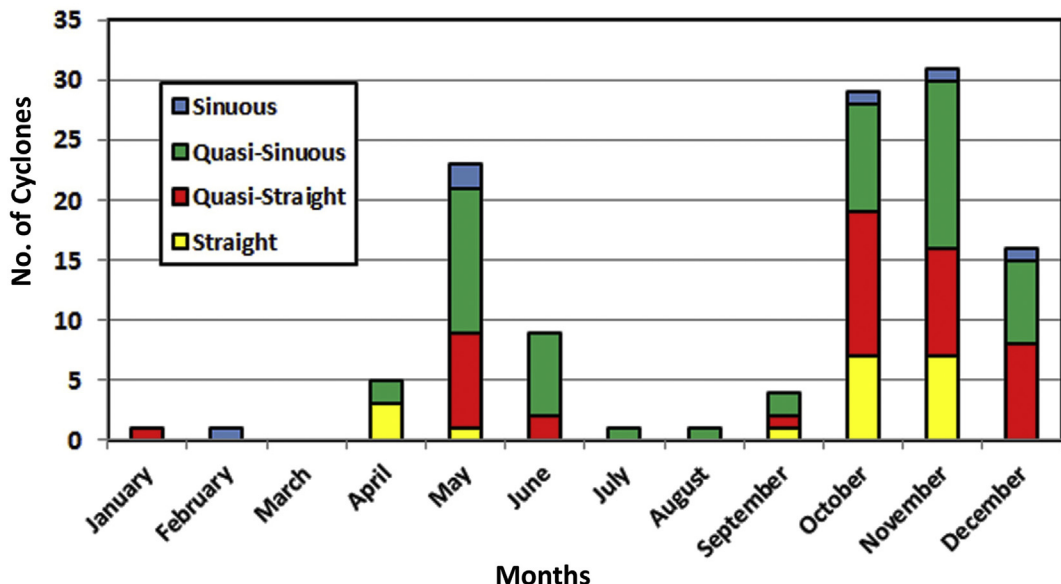


Fig. 10. Month-wise cyclonic track categories over BOB basin during 1971–2020.

The other way to express the details gives an example of how track sinuosity usually varies during the cyclone season, i.e. exemplifies track type seasonality. This is done by sorting the entire SI dataset into transformed categories of 'straight' and 'quasi-straight' and even integrated groups of 'quasi-sinuous' and 'sinuous', and then plotting the data according to the month in which actual cyclones were spawned during 1971–2020 (Fig. 10). Fig. 8 immediately shows that late cyclone season months (October to December) tend to produce a higher proportion of straighter tracks and forms nearly 63 per cent of cyclonic events. Notably, tracks then undergo a marked change at the height of the season, dominated by May with a much higher percentage of 'quasi-straight' and 'quasi-sinuous' shape tracks (17 per cent). The proportions of cyclones with either quasi-sinuous or sinuous paths then become nearly equal for the latter months of the cyclone season (February to April). It can be supposed that, since the cyclones appear to travel in quasi-straight directions, the migration of such cyclones spawned in the later phase of any given season should be more consistent.

## 6. Summary and conclusion

The current research is an effort to establish a long-term climate science BoB TCs for the duration 1971–2020 based on the RSMC-IMD dataset. A total of 121 TCs with an average of 35.2 TCs per decade were developed in the BoB without any significant increasing or decreasing trend. Likewise, in their VF, ACE and PDI values, non-significant rising or decreasing patterns were observed which has a significant relation with ENSO phenomena. In all parts of the BoB, TCs were produced and made their landfall across the coasts of India, Bangladesh, Myanmar and Sri Lanka. A wide variation in genesis positions and tracks was observed during two peak TC seasons (pre- and

post-monsoon seasons). Most of the TCs took the northward track during the pre-monsoon season and made their landfall across the coasts of Bangladesh and Myanmar, while post-monsoon TCs made their landfall directly on the coasts of Orissa and West Bengal. From the month of April to July, the mean location of TCs in genesis shifts northward and then continuously pushes southward. Even though the average distance covered by post-monsoon TCs was higher than that in the pre-monsoon season, and the maximum TCs ranged from 800 to 2300 km. ENSO and its relation to TC behaviour in the BoB during the primary TC peak season were studied during the period 1982–2020. The results show that ENSO significantly influences the frequency, position of genesis and intensity of TC during the primary TC peak season in the BoB. TC activity is comparatively more and less pronounced during La Niña and El Niño regimes respectively and the genesis position in the BoB is moved to the east (west) of 87° E. During the cold regime, the number of extreme TC events, above the VSCS category, increased intensely in the BoB.

During the post-monsoon season and year as a whole, when comparing the energy metrics over the BoB, the VF, ACE and PDI of TCs are significantly higher over BoB. VF, ACE and PDI are significantly higher in post monsoon phase than in the monsoon season, in case of TCs and higher in the pre-monsoon season than in the monsoon season in the case of TCs over the BoB as a whole year, while comparing the energy metrics in different seasons. While the annual VF and PDI are more dependent on intensity per year, ACE depends more, but similarly, on the speed and duration of TC over the BoB. All the above three measurements are significantly least conditional on the TC incidence of propagation over BoB. This relationship changes, however, as we regard BoB in separate seasons. In post-monsoon seasons with both La Niña conditions, the VF, ACE and PDI over the BoB are substantially

higher than that with El Niño conditions. This combined effect does not, however, affect the BoB during the pre-monsoon season. During the pre-monsoon season, there is a major decreasing trend in VF, ACE and PDI of TCs over BoB, mainly due to similar trends in the average intensity of TCs.

Here in the Bay of Bengal, the sinuosity of 121 tropical cyclone tracks was calculated using a proven technique that was successfully used in the BoB basin. Sinuosity is an easy term to grasp, a convenient metric to represent the shape of cyclone tracks, which can be quantified for both simple and convoluted forms of tracks with the same degree of accuracy. It is possible to highlight some key results from the study. Firstly, according to their sinuosity group, mapping cyclone tracks helps to show which areas of the BoB are more responsive to networks following easy or meandering directions. Secondly, with regard to the long-term picture, there is a statistically significant downward trend seen in the sinuosity of the track. However, because of incremental improvements in operating procedures in the BoB basin, as stated earlier, this trend may be exaggerated or spurious. A third finding is that there is often significant seasonal and inter-annual variability in track sinuosity (as in other basins), indicating that unpredictable conditions will continue in the future. Crucially, however, there are clearly known numerous noticeable instances of magnified or weakened track sinuosity, often lasting several years. It is believed that the research findings will help the scientific community, Disaster Management Group of the nation and other stakeholders to take accurate strides to combat such violent events with persistent intensification.

## Declaration of competing interest

The authors declare that they have no known competing financial interests or personal relationships that could have appeared to influence the work reported in this paper.

## Acknowledgements

The authors are also thankful to RSMC-IMD, New Delhi for giving them access to the required data used in this study. Two anonymous referees are thanked for providing constructive comments on the original manuscript submission. This work has been supported by the Ministry of Science and Technology & Biotechnology (WBDSTBT), Govt. of West Bengal, India Vide Memo. ST/P/S&T/5G-12/2018 dated February 25, 2019.

## Appendix A. Supplementary data

Supplementary data to this article can be found online at <https://doi.org/10.1016/j.tctr.2021.11.004>.

## References

Anandh, T.S., Das, B.K., Kuttippurath, J., Chakraborty, A., 2020. A coupled model analyses on the interaction between oceanic eddies and tropical

cyclones over the Bay of Bengal. *Ocean Dynam.* 70, 327–337. <https://doi.org/10.1007/s10236-019-01330-x>.

Bhardwaj, P., Singh, O., 2019. Climatological characteristics of Bay of Bengal tropical cyclones: 1972–2017. *Theor. Appl. Climatol.* 139, 615–629. <https://doi.org/10.1007/s00704-019-02989-4>.

Balaguru, K., Leung, L.R., Lu, J., Foltz, G.R., 2016. A meridional dipole in premonsoon Bay of Bengal tropical cyclone activity induced by ENSO. *J. Geophys. Res. Atmos.* 121, 6954–6968.

Bhardwaj, P., Pattaik, D.R., Singh, O., 2019. Tropical cyclone activity over Bay of Bengal in relation to El Niño-southern oscillation. *Int. J. Climatol.* 39 (4), 1–18. <https://doi.org/10.1002/joc.6165>.

Biswas, H.R., Kundu, P.K., 2018. A principal component analysis based model to predict post-monsoon tropical cyclone activity in the Bay of Bengal using oceanic Niño index and dipole mode index. *Int. J. Climatol.* 38, 2415–2422.

Chen, J., Mueller, V., 2018. Coastal climate change, soil salinity and human migration in Bangladesh. *Nat. Clim. Chang.* 8, 981–985. <https://doi.org/10.1038/s41558-018-0313-8>.

Colbert, A.J., Soden, B.J., 2012. Climatological variations in North Atlantic tropical cyclone tracks. *J. Clim.* 25, 657–673.

Cutter, S.L., Finch, C., 2008. Temporal and spatial changes in social vulnerability to natural hazards. *Proc. Natl. Acad. Sci.* 107, 2301–2306.

Down To Earth, 2020. Less atmospheric aerosol may have intensified Cyclone Amphan. <https://www.downtoearth.org.in/news/climate-change/-less-atmospheric-aerosol-may-have-intensified-cyclone-amphan-71280>.

Dube, S.K., Rao, A.D., Sinha, Murty, T.S., Bahulayan, H., 1997. Storm surge in the Bay of Bengal and Arabian Sea: the problem and its prediction. *Mausam* 48 (2), 283–304.

Emanuel, K., 2005. Increasing destructiveness of TCs over the past 30 years. *Nature* 436 (7051), 686–688.

Fang, J., Sun, S., Shi, P., Wang, J., 2014. Assessment and mapping of potential storm surge impacts on global population and economy. *Int. J. Disaster Risk. Sci.* 5, 323–331. <https://doi.org/10.1007/s13753-014-0035-0>.

Girishkumar, M.S., Suprit, K., Vishnu, S., Prakash, T.V.P., Ravichandran, M., 2015. The role of ENSO and MJO on rapid intensification of tropical cyclones in the Bay of Bengal during October–December. *Theor. Appl. Climatol.* 120, 797–810.

Karmakar, K., Hassan, S.M.Q., 2004. Unusual behaviour of a tropical cyclone over the Bay of Bengal and comparison of its different tracks. In: Proceedings of the SAARC Seminar on Tropical Cyclones & Storm Surges in the South Asian Region, 20–22 December 2003, Published by SMRC in 2004. Accessed through. <https://www.researchgate.net/publication/283344059>.

Kumar, P., Geneletti, D., Nagendra, H., 2016. Spatial assessment of climate change vulnerability at city scale: a study in Bangalore, India. *Land Use Pol.* 58, 514–532. <https://doi.org/10.1016/j.landusepol.2016.08.018>.

Lander, M.A., 1994. An exploratory analysis of the relationship between tropical storm formation in the western North Pacific and ENSO. *Mon. Weather Rev.* 122, 636–651.

Lindeboom, W., Alam, N., Begum, D., Kim-Streatfield, P., 2012. The association of meteorological factors and mortality in rural Bangladesh, 1983–2009. *Glob. Health Action* 5 (1), 19063.

Liou, Y.A., Nguyen, A.K., Li, M.H., 2017. Assessing spatiotemporal eco-environmental vulnerability by Landsat data. *Ecol. Indic.* 80, 52–65. <https://doi.org/10.1016/j.ecolind.2017.04.055>.

Marín-Monroy, E.A., Trejo, V.H., Pena, M., Polanco, G.A., Barbara, N.L., 2020. Assessment of socio-environmental vulnerability due to tropical cyclones in La Paz, Baja California Sur, Mexico. *Sustainability* 12, 1575. <https://doi.org/10.3390/su12041575>.

Mohapatra, M., Kumar, M.M., 2015. Interannual variation of tropical cyclone energy metrics over North Indian Ocean. *Clim. Dyn.* 48, 1431–1445. <https://doi.org/10.1007/s00382-016-3150-3>.

Mousavi, M.E., Irish, J.L., Frey, A.E., Olivera, F., Edge, B.L., 2010. Global warming and hurricanes: the potential impact of hurricane intensification and sea level rise on coastal flooding. *Clim. Change.* <https://doi.org/10.1007/s10584-009-9790-0>.

Nath, S., Kotal, S.D., Kundu, P.K., 2016. Decadal variation of ocean heat content and tropical cyclone activity over the Bay of Bengal. *J. Earth Syst. Sci.* 125, 65–74.

- Neumann, C.J., 1993. Global Overview. Global Guide to Tropical Cyclone Forecasting. WMO/TD-560 World Meteorological Organization, pp. 1.1–1.42.
- Ng, E.K.W., Chan, J.L.C., 2012. Inter annual variations of tropical cyclone activity over the north Indian Ocean. *Int. J. Climatol.* 32, 819–830.
- Oo, A.T., Huylenbroeck, V.G., Speelman, S., 2018. Assessment of climate change vulnerability of farm households in Pyapon District, a delta region in Myanmar. *Int. J. Disaster Risk Reduct.* 28, 10–21.
- Pandey, R.S., Liou, Y.A., 2020. Decadal behaviors of tropical storm tracks in the north west Pacific ocean. *Atmos. Res.* 246, 105143. <https://doi.org/10.1016/j.atmosres.2020.105143>.
- Pattanaik, D.R., 2005. Variability of oceanic and atmospheric conditions during active and inactive periods of storms over the Indian region. *Int. J. Climatol.* 25, 1523–1530.
- Rabby, Y.W., Hossain, M.D.B., Hasan, M.U.I., 2019. Social vulnerability in the coastal region of Bangladesh: an investigation of social vulnerability index and scalar change effects. *Int. J. Disaster Risk Reduct.* 41, 101329.
- Rao, Y.P., 1976. Southwest monsoon. Met. Monograph No.1/1976, 107–185.
- Rehman, S., Sahana, M., Kumar, P., Ahmed, R., Sajjad, H., 2020. Assessing hazards induced vulnerability in coastal districts of India using site specific indicators: an integrated approach. *Geojournal* 1–22.
- Sahana, M., Sajjad, H., 2019. Vulnerability to storm surge flood using remote sensing and GIS techniques: a study on Sundarban biosphere reserve, India. *Remote Sens. Appl. Soc. Environ.* 13, 106–120.
- Sahana, M., Hong, H., Ahmed, R., Patel, P.P., Bhakat, P., Sajjad, H., 2019. Assessing coastal island vulnerability in the Sundarban Biosphere Reserve, India, using geospatial technology. *Environ. Earth Sci.* 78 (10), 304.
- Schreck, C.J., Knapp, K.R., Kossin, J.P., 2014. The impact of best track discrepancies on global tropical cyclone climatologies using IBTrACS. *Mon. Weather Rev.* 142 (10), 3881–3899.
- Sengupta, D., Goddalehundi, B.R., Anitha, D.S., 2007. Cyclone induced mixing does not cool SST in the post-monsoon north Bay of Bengal. *Atmos. Sci. Lett.* 9, 1–6.
- Siddiqui, M.R., 2014. Patterns and factors of natural hazard induced out-migration from Meghna Estuarine Islands of Bangladesh. *GeoScape* 8, 17–31.
- Singh, O.P., 2008. Indian Ocean dipole mode and tropical cyclone frequency. *Curr. Sci.* 94, 29–31.
- Singh, O.P., Khan, T.M.A., Rahman, M.S., 2001a. Probable reasons for enhanced cyclogenesis in the Bay of Bengal during July–August of ENSO years. *Glob. Planet. Change* 29 (1–2), 135–147.
- Singh, O.P., Khan, T.M.A., Rahman, M.S., 2001b. Has the frequency of intense tropical cyclones increased in the north Indian Ocean? *Curr. Sci.* 80 (4), 575–580.
- Terry, J.P., Feng, C.C., 2010. On quantifying the sinuosity of typhoon tracks in the western North Pacific basin. *Appl. Geogr.* 30, 678–686.
- Terry, J.P., Gienko, G., 2011. Developing a new sinuosity index for cyclone tracks in the tropical South Pacific. *Nat. Hazards* 59, 1161–1174.
- Terry, J.P., Gienko, G., 2018. Quantitative observations on tropical cyclone tracks in the Arabian Sea. Theoretical and applied climatology. *Theor. Appl. Climatol.* <https://doi.org/10.1007/s00704-018-2445-1>.
- Terry, J.P., Kim, I.H., 2015. Morphometric analysis of tropical storm and hurricane tracks in the North Atlantic basin using a sinuosity-based approach. *Int. J. Climatol.* 35, 923–934.
- Terry, J.P., Kim, I.H., Jolivet, S., 2013. Sinuosity of tropical cyclone tracks in the South West Indian Ocean: spatio-temporal patterns and relationships with fundamental storm attributes. *Appl. Geogr.* 45, 29–40.
- The Hindu, 2020. Cyclone amphan batters West Bengal, Odisha. <https://www.thehindu.com/news/national/other-states/cyclone-amphan-batters-west-bengal-odisha/article31634110.ece>.
- Wang, B., Chan, J.C.L., 2002. How strong ENSO events affect tropical storm activity over the western North Pacific? *J. Clim.* 15 (15), 1643–1658. [https://doi.org/10.1175/1520-0442\(2002\)015](https://doi.org/10.1175/1520-0442(2002)015).
- Wang, C., Wang, X., Weisberg, R.H., Black, M.L., 2017. Variability of tropical cyclone rapid intensification in the North Atlantic and its relationship with climate variations. *Clim. Dyn.* 49, 3627–3645.
- Zhang, W., Leung, Y., Chan, J.C.L., 2013. The analysis of tropical cyclone tracks in the Western North Pacific through data mining. Part I: tropical cyclone recurvature. *J. Appl. Meteorol. Climatol.* 52, 1394–1416.